Available online at www.sciencedirect.com
SCIENCE DIRECT®
Inorganica Chimica Acta 345 (2003) 299–308
Inorganica Chimica Acta
www.elsevier.com/locate/ica

Synthesis of 1,2-bis(di-*tert*-butylphosphino)ethane (dtbpe) complexes of nickel: radical coupling and reduction reactions promoted by the nickel(I) dimer $[(dtbpe)NiCl]_2$

Daniel J. Mindiola [a], Rory Waterman [a], David M. Jenkins [b], Gregory L. Hillhouse [a,*]

[a] *Department of Chemistry, Searle Chemistry Laboratory, The University of Chicago, Chicago, IL 60637, USA*
[b] *Division of Chemistry and Chemical Engineering, California Institute of Technology, Pasadena, CA 91125 USA*

Received 13 June 2002; accepted 3 August 2002

Dedicated to our friend Professor Richard R. Schrock, an inspiring master of synthetic organometallic chemistry and catalysis

Abstract

Tetrahydrofuran solutions of $(dtbpe)NiCl_2$ (dtbpe = 1,2-bis(di-*tert*-butylphosphino)ethane) are reduced by KC_8 to afford the dimeric Ni(I) complex $[(dtbpe)NiCl]_2$ (**1**) in 73% yield. Reaction of **1** with $[FeCp_2][PF_6]$ effects a one-electron oxidation to give the mixed-valent Ni(I,II) binuclear species $[\{(dtbpe)NiCl\}_2][PF_6]$, **[1][PF$_6$]**. Complex **1** reacts with the radicals NO and TEMPO (2,2,6,6-tetramethyl-1-piperidine-*N*-oxyl) to give the diamagnetic Ni(0) nitrosyl (dtbpe)Ni(Cl)(NO) (**2**) and the Ni(II) complex (dtbpe)Ni(Cl)(O,N:η^2-TEMPO) (**3**). Reduction of the S–S bond of diphenyldisulfide by **1** results in formation of the Ni(II) arylthiolate complex (dtbpe)NiCl(SPh) (**4**). The radical anions $NaOCPh_2$ and KN_2Ph_2 react cleanly with **1** to afford (dtbpe)Ni(η^2-$OCPh_2$) (**5**) and (dtbpe)Ni(η^2-N_2Ph_2) (**6**). Phenylacetylide C–C bond coupling is effected by reaction of **1** with LiC≡CPh to form $[(dtbpe)Ni(C,C':\eta^2\text{-}CCPh)]_2$ (**7**). In addition to standard spectroscopic (IR, NMR, EPR) and magnetic measurements, complexes **1**, **[1][PF$_6$]**, **3**, and **5** were also characterized by single-crystal X-ray diffraction methods.

Keywords: Crystal strcutures; Nickel complexes; Diphosphine complexes; Dimeric complexes

1. Introduction

Well-defined Ni(I) complexes are relatively rare [1], yet this unusual oxidation state has been invoked in biologically relevant processes involving nickel-containing enzymes such as hydrogenase, carbon monoxide dehydrogenase, and methyl-*S*-coenzyme M reductase [2]. It is appreciated that the catalytic activity of these nickel enzymes is dependent on redox processes involving the nickel center [2]. Isolation of homogeneous complexes supporting the Ni(I) oxidation state are interesting in that they offer the opportunity to study and understand reactivity associated with an unusual oxidation state. Monomeric Ni(I) complexes are expected to be paramagnetic (d^9 electron configuration) and to demonstrate redox properties unique to a Group 10 radical. Work in our laboratories has shown that electron rich Ni(I) complexes can readily incorporate hard ligands without reduction or disproportionation, affording excellent platforms for novel metal–ligand multiple bonds [1n,q]. The use of bulky substituents on the tertiary, chelating phosphorus ligand of 1,2-bis(di-*tert*-butylphosphino)ethane (dtbpe) has allowed us to develop a synthetic route to a stable Ni(I) chloride complex and to explore its spectroscopic properties and redox and substitution chemistry, topics presented in this contribution.

* Corresponding author. Tel.: +1-773-702 7057; fax: +1-773-702 0805
E-mail address: g-hillhouse@uchicago.edu (G.L. Hillhouse).

0020-1693/02/$ - see front matter
PII: S0020-1693(02)01302-6

2. Results and discussion

2.1. Synthesis and reactions of [(dtbpe)NiCl]$_2$

Cold THF solutions of (dtbpe)$NiCl_2$ react in a 1:1 stoichiometry with KC_8 over a period of 2 h to afford [(dtbpe)NiCl]$_2$ (**1**) as large red blocks in 73% yield (Eq. (1)). Related Ni(I) chloride dimers containing chelating diphosphine ligands have been previously reported [1l,n]. Complex **1** is soluble in most common organic solvents such as benzene, Et_2O, and THF, but only sparingly soluble in alkanes. It exhibits reasonable thermal stability in solution and in the solid-state, but upon exposure to oxidants (e.g. O_2) or halogenated solvents (CH_2Cl_2) it gradually decomposes to myriad products. In the solid-state, **1** is a dimer as shown by X-ray crystallography (Fig. 1, Section 2.1.1). Temperature-dependent solid-state magnetic susceptibility measurements of a polycrystalline sample of **1** (SQUID, $10 < T < 255$ K) exhibited classic antiferromagnetic coupling of the two d^9 Ni centers ($T_{max} = 32$ K; $J = -35$ cm^{-1}, $\mu_{max} = 2.25\mu_B$ at 105 K) illustrated in the plot of molar susceptibility (χ_M) as a function of T shown in Fig. 2. Solutions of **1** show an effective magnetic moment of $2.29\mu_B$ per nickel, indicative of either dimer dissociation to give a monomeric structure in solution, or a dimeric structure in which the unpaired electrons are localized on the two metal centers with negligible coupling. The dimeric Ni(I) hydride [(dtbpe)Ni(μ-H)]$_2$, which has a Ni–Ni bond, displays diamagnetic behavior in solution [1r]. The molecular weight of **1** in THF solution (530 amu; avg of two trials), determined using the Signer method, is most consistent with a monomeric solution structure (monomer, 413 amu; dimer, 826 amu), although a weak ion for the dimer can be detected in an electrospray mass spectrum of **1** (824 [M^+]). The room temperature X-band EPR solution spectrum of **1** is a triplet with hyperfine coupling to *2* equivalent phosphorus nuclei (Fig. 3, Section 3.2.1). Although paramagnetic, **1** shows relatively sharp resonances in its ^{1}H NMR spectrum (C_6D_6) which are easily assigned to the *tert*-butyl and methylene groups on the dtbpe ligand.

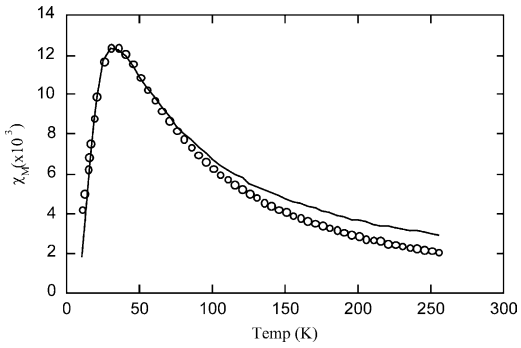

Fig. 2. SQUID data (circles) and calculated fit (line) for **1**. Temp = 10–255 K, $T_{max} = 32$ K; $J = -35$ cm^{-1}; $\mu_{max} = 2.25\mu_B$ at 105 K; fit with $g = 2.05$.

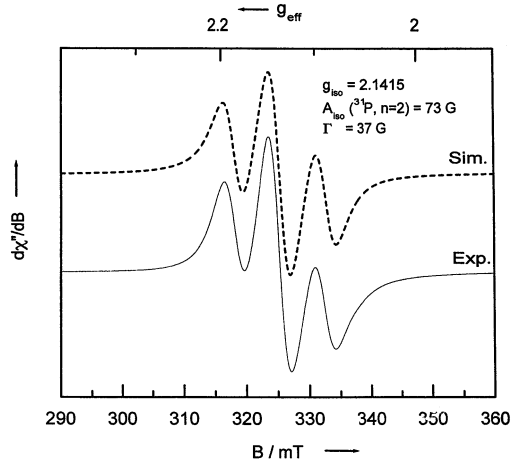

Fig. 3. Room temperature X-band EPS spectrum of **1**.

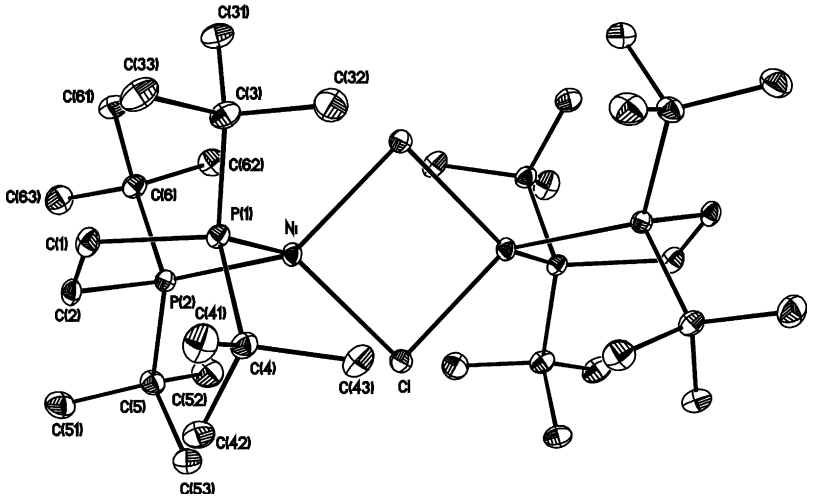

Fig. 1. A perspective view of **1** with thermal ellipsoids at the 35% probability level. Selected bond lengths (Å) and angles (°) are listed in Table 2.

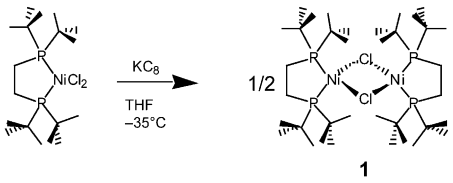

(1)

$[Cp_2Fe][PF_6]$ oxidizes **1** to the purple, paramagnetic species $[\{(dtbpe)NiCl\}_2][PF_6]$, **[1][PF$_6$]**, in good yield (Scheme 1). Solution magnetic susceptibility measurements are consistent with one unpaired electron for the binuclear complex, and the room temperature solution (THF) X-band EPR spectrum indicates one unpaired electron localized about one of the NiP_2 fragments (Fig. 4). Solid-state magnetic measurements (SQUID) showed Curie–Weiss behavior for **[1][PF$_6$]** between 60 and 300 K with $\mu_{avg} = 1.96\mu_B$ consistent with a mixed valence state dimer. The dimeric nature of **[1][PF$_6$]** was confirmed by X-ray crystallography (Fig. 5, Section 2.1.2). Mixed valent Ni(I)/Ni(II) species have been reported for a series of cluster-type frameworks [3]. Complex **[1][PF$_6$]** is stable in the solid-state in the absence of oxidants. However, CH_2Cl_2 solutions containing the dimer gradually decompose over several days to a complex mixture that includes several uncharacterized diamagnetic products.

Treatment of **1** with 1 equiv./Ni of radicals such as nitric oxide (NO) and TEMPO (2,2,6,6-tetramethyl-1-piperidine-*N*-oxyl) affords the monomeric, diamagnetic, and formally Ni(0) nitrosyl complex (dtbpe)NiCl(NO) (**2**; 80% yield) and the monomeric, diamagnetic Ni(II) complex (dtbpe)Ni(Cl)(O,N:η^2-TEMPO) (**3**; 90% yield), respectively (Scheme 1). Complexes **2** and **3** were characterized by multinuclear NMR (^{1}H, ^{13}C, ^{31}P) and IR spectroscopies, and elemental analysis. The ^{1}H NMR spectrum of complex **2** shows two distinct sets of doublets for the *tert*-butyl protons on the dtbpe ligand,

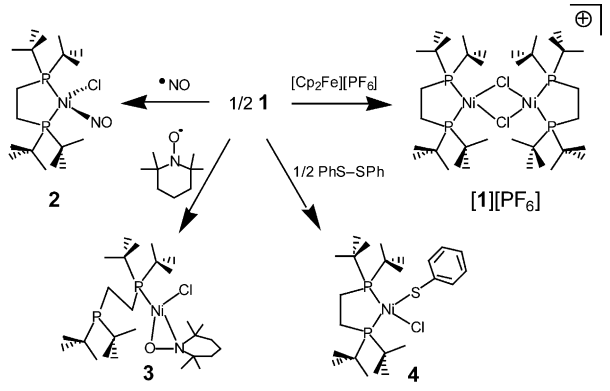

Scheme 1. Oxidation of **1** with 1 equivalent of $[Cp_2Fe][PF_6]$ in cold THF provides **[1][PF$_6$]** as large purple blocks in 94% yield. Complex **1** couples with the radical NO in cold toluene solutions to afford **2** in 80% yield as large blue blocks. Addition of TEMPO to **1** in toluene affords **3** in 90% yield as large purple blocks. Complex **1** slowly reduces PhSSPh (24 h) in toluene to afford large brown blocks on **4** in 60% yield.

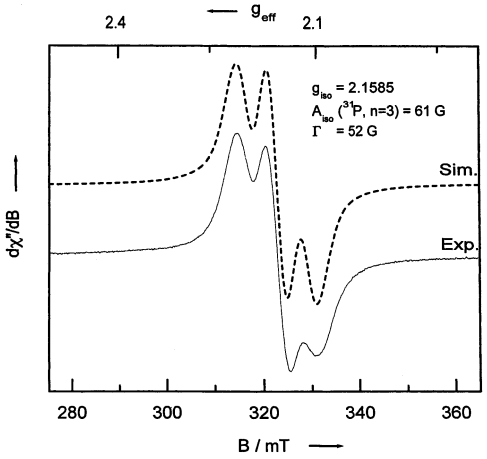

Fig. 4. Room temperature X-band EPR spectrum of **[1][PF$_6$]**.

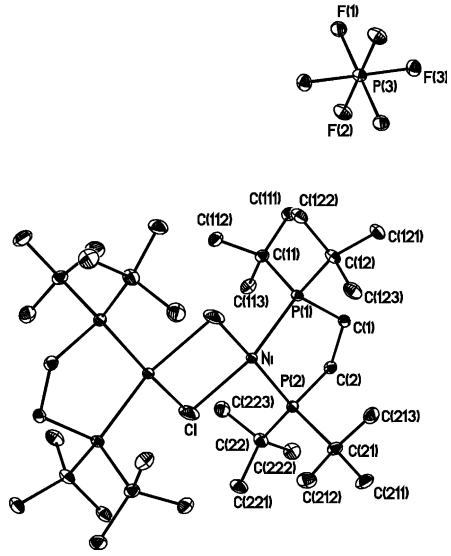

Fig. 5. A perspective view of **[1][PF$_6$]** with thermal ellipsoids at the 35% probability level. Selected bond lengths (Å) and angles (°) are listed in Table 2.

while the ^{31}P NMR spectrum indicates 1 equivalent phosphorus environment, data consistent with **2** possessing pseudotetrahedral coordination geometry. The IR spectrum of blue, crystalline **2** shows a strong ν(NO) at 1734 cm^{-1}, a value similar to that found in other d^{10}, Ni(0) complexes containing linear nitrosyl ligands [4]. Ether solutions containing the TEMPO radical react rapidly with **1** to afford purple solutions from which **3** can be isolated. NMR spectra (^{1}H and ^{31}P) indicate inequivalent phosphorus nuclei, consistent with either an η^1-O-bound TEMPO ligand [5] or a complex having an η^2-O,N-bound TEMPO ligand (its most common binding mode in metal complexes) [5,6] and a monodentate dtbpe ligand in which one phosphine arm has dissociated from nickel. In order to differentiate between these two possibilities, we determined the solid-state molecular structure of **3** by single crystal X-ray

diffraction methods and showed the latter structure with a fully reduced, η^2-*O*,*N*-bound TEMPO ligand to be the correct one (Section 2.1.3).

Addition of 1 equivalent of diphenyldisulfide to **1** in toluene solution slowly effects reduction of the S–S bond to afford the Ni(II) complex (dtbpe)NiCl(SPh) (**4**) as dark brown blocks in 60% yield (Scheme 1). ^{1}H and ^{31}P NMR data are in accordance with a square-planar Ni(II) complex containing mutually *cis* chloride and phenylthiolato ligands, demonstrating the reducing ability of Ni(I) complexes supported by electron rich phosphine ligands. Analogous dichalcogenide bond reductions by metalloradicals are known, for example, in the chemistry of divalent lanthanides [7].

Treatment of **1** with the stable radical anions of benzophenone ($Ph_2CO^{\bullet -}$) and azobenzene ($Ph_2N_2^{\bullet -}$) afforded the diamagnetic adducts (dtbpe)Ni(η^2-$OCPh_2$) (**5**; 88% yield) and (dtbpe)Ni(η^2-N_2Ph_2) (**6**; 84% yield), respectively (Scheme 2) [8]. While it is common for ketones and 1,2-disubstituted diazenes to react with Ni(0) complexes to afford Ni(II) η^2-adducts [9], substitution and radical coupling reactions effected by a Ni(I) complex, analogous to those reported here, have not been previously reported. The high reduction potential of **1** suggests that both complexes **5** and **6** are likely generated by transmetallation and radical coupling (or vice versa) rather than by reduction of Ni(I) to Ni(0) via electron transfer followed by binding of the neutral ketone or azobenzene. Complexes **5** and **6** were characterized by multinuclear NMR (^{1}H, ^{13}C, ^{31}P) spectroscopy and elemental analysis. The ^{1}H NMR spectrum of **5** revealed equivalent phenyl groups on the ketone ligand while the ^{31}P NMR spectrum indicated inequivalent phosphorus nuclei consistent with a square-planar geometry about the nickel center. This was confirmed by X-ray crystallography (Section 2.1.4).

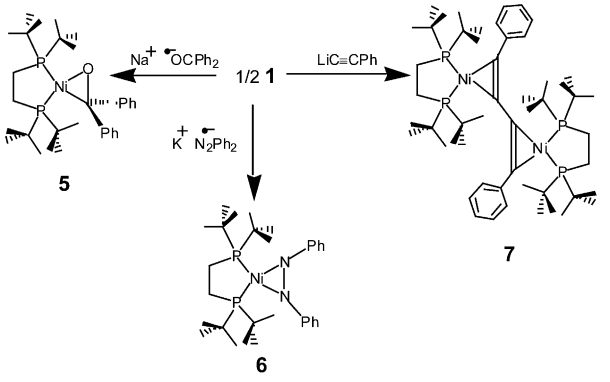

Scheme 2. Addition of cold THF solutions containing the radical anion $NaOCPh_2$ to **1** affords **5** in 96% yield, as orange plates. Similarly, addition of **1** to cold THF solutions containing the radical anion KN_2Ph_2 provides **6** as dark red plates in 84% yield. Metathesis of **1** with LiC≡CPh in Et_2O gives **7** in 94% yield as yellow–orange blocks.

Likewise, NMR spectra of **6** indicate a similar square-planar geometry for this complex.

When an Et_2O slurry of **1** is treated with LiC≡CPh, a yellow solution results from which a complex (**7**) of the empirical formula '(dtbpe)Ni(C_2Ph)' can be isolated in 94% yield (Scheme 2). We have prepared a variety of 'three-coordinate' Ni(I) alkyls supported by the dtbpe ligand, and when the alkyl substituent is sufficiently bulky, they are monomeric, paramagnetic d^9 species [10]. However, **7** is diamagnetic with two sets of inequivalent dtbpe *tert*-butyl groups, two inequivalent phosphorus environments (^{31}P NMR), and an olefinic stretch at 1589 cm^{-1} in the infrared. Based on these spectroscopic data and their similarity to those for (dtbpe)Ni{*C*,*C*′:η^2-C(Ph)C(H)} [11] and other η^2-acetylene complexes of Ni [12], we formulate **7** as an η^2-actetylene-coupled dimer, [(dtbpe)Ni(*C*,*C*′:η^2-CCPh)]$_2$ [13]. The dimer is probably formed from radical coupling of the initial Ni(I) product of metathesis, (dtbpe)Ni(C≡CPh). It is noteworthy that we do not observe (dtbpe)Ni(C≡CPh)$_2$ as a product in the reaction, even though when not prohibited by sterics, disproportionation of Ni(I) alkyls (i.e. $L_xNi(R)$) to Ni(II) bisalkyl complexes ($L_xNi(R)_2$) and 'Ni(0)' is common [10].

2.1.1. Molecular structure determination of *1*

Previous workers describing the synthesis of Ni(I) halide complexes supported by chelate phosphines speculated that such systems could be either monomeric or dimeric in solution depending on the steric bulk of the supporting phosphine [11]. X-ray structural analysis of **1** provided the first metrical parameters for a Ni(I) halide complex supported by phosphines. Diffraction quality crystals of **1** were grown from a dilute Et_2O solution cooled to −35 °C. A perspective view of **1** is shown in Fig. 1. Table 1 gives crystal information and data collection and refinement parameters for the structural analysis. Selected bond distances and angles for **1** can be found in Table 2.

The structure of **1** shows a binuclear Ni(I) species bridged by chloride ligands. An inversion center about the Ni_2Cl_2 centroid relates each metal fragment in the complex giving the molecule D_{2h} point symmetry. Each nickel center adopts a pseudotetrahedral geometry with the {P, Ni, P} and {Cl, Ni, Cl} planes being nearly orthogonal. The Ni–Cl–Ni bridges are slightly asymmetric, with Ni–Cl distances of 2.3507(8) and 2.3858(8) Å.

2.1.2. Molecular structure determination of *[1][PF$_6$]*

Single violet plates of X-ray quality of complex [**1**][PF_6] can be readily grown at −35 °C from a CH_2Cl_2 solution layered with Et_2O. A molecular view of [**1**][PF_6] is shown in Fig. 5. It is interesting that removal of one electron from pseudotetrahedral **1** forces

Table 1
Crystallographic data

Compound	**1**	[**1**][PF_6]	**3**	**5**
Empirical formula	$C_{18}H_{40}ClNiP_2$	$C_{18}H_{40}ClF_3NiP_{2.5}$	$C_{27}H_{58}ClNNiOP_2$	$C_{31}H_{50}NiOP_2$
Formula weight	412.60	485.08	568.84	559.36
Space group	*C*2/*c*	$P2_1/c$	$P2_1/c$	*C*2/*c*
a (Å)	23.356(5)	13.3329(9)	10.7705(11)	17.872(7)
b (Å)	16.378(4)	11.3782(8)	27.412(3)	16.253(7)
c (Å)	12.316(3)	16.5264(12)	11.2806(12)	21.135(9)
β (°)	114.762(4)	110.9020(10)	111.434(2)	101.131(8)
V (Å^3)	4278.2(16)	2342.1(3)	3100.2(6)	6024(4)
Z	8	4	4	8
D_{calc} (Mg m^{-3})	1.281	1.376	1.219	1.234
μ (mm^{-1})	1.178	1.137	0.834	0.772
F(000)	1784	1030	1240	2416
Crystal color, form	pale yellow	violet	violet	orange
Crystal form	block	plate	needle	block
Crystal size (μm)	200 × 160 × 80	300 × 300 × 40	210 × 200 × 100	80 × 60 × 20
θ Range (lattice, °)	1.57–28.37	1.63–28.30	2.16–28.30	1.71–28.44
Index ranges	$-30 \le h \le 30$, $-21 \le k \le 21$, $-16 \le l \le 15$	$-17 \le h \le 17$, $-15 \le k \le 6$, $-21 \le l \le 21$	$-8 \le h \le 14$, $-35 \le k \le 34$, $-15 \le l \le 14$	$-18 \le h \le 23$, $-21 \le k \le 20$, $-26 \le l \le 27$
Reflections collected	25 046	14 056	18 912	18 193
Independent reflections (R_{int} [a])	5164(0.0559)	5503(0.0454)	7240(0.0553)	7126(0.0834)
Data/restraints/parameters	5164/0/199	5503/0/233	7240/0/298	7126/0/316
Final *R* indices [$I > 2\sigma(I)$] [c]	$R_1 = 0.0417$, $wR_2 = 0.0840$	$R_1 = 0.0432$, $wR_2 = 0.0972$	$R_1 = 0.0438$, $wR_2 = 0.0755$	$R_1 = 0.0802$, $wR_2 = 0.1767$
R indices (all data) [d]	$R_1 = 0.0525$, $wR_2 = 0.0880$	$R_1 = 0.0477$, $wR_2 = 0.0999$	$R_1 = 0.0668$, $wR_2 = 0.0810$	$R_1 = 0.1172$, $wR_2 = 0.3271$
Goodness-of-fit on F^2 [b]	1.115	1.164	0.876	1.092
Largest difference peak and hole (e Å^{-3})	0.557 and −0.393	0.695 and −0.406	0.616 and −0.415	1.305 and −0.555

Common features to all crystals: monoclinic ($\alpha = \gamma = 90°$), $T = 100$ K, Wavelength = 0.71073 Å. Refinement method: Full-matrix least-squares on F^2, Absorption correction: semi empirical from psi-scans.

[a] $\text{Rint} = \Sigma\ |F_o^2 - \langle F_o^2 \rangle| / \Sigma\ |F_o^2|$.

[b] Goodness-of-fit $= S = [\Sigma\ [w(F_o^2 - F_c^2)^2] / (n-p)]^{1/2}$.

[c] $R_1 = \Sigma\ ||F_o| - |F_c|| / \Sigma\ |F_o|$.

[d] $wR_2 = [\Sigma\ [w(F_o^2 - F_c^2)^2] / \Sigma\ [w(F_o^2)^2]]^{1/2}$ for: $w = q/\sigma^2(F_o^2) + (aP)^2 + bP$, n = number of independent reflections, p = number of parameters refined, and weighting scheme $w = q[\sigma^2(F_o^2) + (aP)^2 + bP]^{-1}$ where: $P = (F_o^2 + 2F_c^2)/3$, $a =$, $b =$, $q = 1$.

the geometry of the nickel centers in [**1**][PF_6] to shift to a square-planar geometry. As in **1**, the chlorides in [**1**][PF_6] also bridge slightly asymmetrically (Ni–Cl = 2.2881(7) and 2.3144(8) Å) with the Ni–Cl bond lengths in [**1**][PF_6] shorter by approximately 0.07 Å than the corresponding distances found in **1**. Fig. 5 shows a perspective view of the salt, with well-separated cations and anions, in which the nickel centers are related by an inversion center. Compiled crystallographic data for [**1**][PF_6] can be found in Table 1, and selected metrical parameters for [**1**][PF_6] can be found in Table 2.

Table 2
Select bond lengths (Å) and angles (°) for **1** and [**1**][PF_6]

	1	[**1**][PF_6]
Bond lengths		
Ni–P(2)	2.2110(7)	2.2223(6)
Ni–P(1)	2.2161(7)	2.2197(6)
Ni–Cl#1	2.3507(8)	2.3144(8)
Ni–Cl	2.3858(8)	2.2881(7)
Bond angles		
P(2)–Ni–P(1)	91.98(3)	91.60(2)
P(1)–Ni–Cl#1	110.25(3)	94.77(2)
P(2)–Ni–Cl#1	131.78(3)	166.32(3)
P(1)–Ni–Cl	129.27(3)	166.38(3)
P(2)–Ni–Cl	110.30(3)	95.18(3)
Cl#1–Ni–Cl	88.36(2)	81.22(3)
Ni#1–Cl–Ni	91.64(2)	98.78(3)

2.1.3. Molecular structure determination structure of **3**

A perspective view of the structure of **3** is shown in Fig. 6 with pertinent bond distances and angles given in the caption. Table 1 gives crystallographic parameters associated with the structural analysis of **3**. The most noteworthy feature of the structure of **3** is the η^2-binding mode of the TEMPO ligand which results in displacement of one arm of the dtbpe ligand. The geometry about the nickel(II) is square-planar with chloride *trans* to oxygen and with the O(1) Ni, N(1), P(2), and Cl atoms nearly coplanar. The Ni–N(1) bond

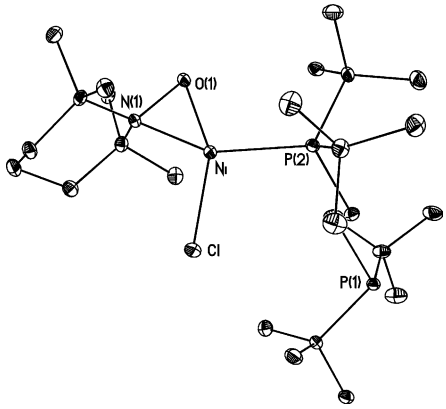

Fig. 6. A perspective view of **3** with thermal ellipsoids at the 35% probability level. Selected bond lengths (Å): Ni–Cl, 2.1780(7); Ni–O(1), 1.839(2); Ni–N(1), 1.926(2), O(1)–N(1), 1.385(2); Ni–P(2), 2.1953(8). Selected angles (°): Cl–Ni–P(2), 99.35(3); N(1)–Ni–Cl, 108.28(6); N(1)–Ni–O(1), 43.08(7); Cl–Ni–O(1), 151.36(6); O(1)–Ni–P(2), 109.19(5).

distance of 1.926(2) Å is typical of a Ni–N single bond, [1n] and the Ni–O(1) bond distance (1.839(2) Å) is similar to that observed in the oxametallacyclopropane moiety of **5** (1.842(3) Å; Section 2.1.4).

2.1.4. *Molecular structure determination of* **5**

Compiled crystallographic data for **5** can be found in Table 1. A perspective view of the structure is shown in Fig. 7, and selected bond lengths and angles are listed in the figure caption. The complex adopts a square-planar geometry in which the ketone is bonded in an η^2-fashion to Ni. The O–C distance of 1.331(6) Å demonstrates the degree of reduction of the ketone versus that for free benzophenone (1.224–1.238 Å) [14]. Similar ketone complexes of nickel supported by phosphine ligands have been prepared and structurally characterized [8]. The solid-state structure of **5** shows no other exceptional features.

3. Experimental

3.1. General considerations

Unless otherwise stated, all operations were performed in a M. Braun Lab Master dry box under an atmosphere of purified nitrogen or using high-vacuum and standard Schlenk techniques under an Ar atmosphere [15]. Hexanes, petroleum ether, and $C_6H_5CH_3$ were dried by passage through activated alumina and Q-5 columns [16]. C_6D_6, and CD_2Cl_2 were purchased form Cambridge Isotope Laboratory (CIL), degassed, and dried over CaH_2 or activated 4 Å molecular sieves. Celite, alumina, and 4 Å molecular sieves were activated under vacuum overnight at a temperature above 180 °C. Anhydrous solvents such as C_6H_6 and Et_2O

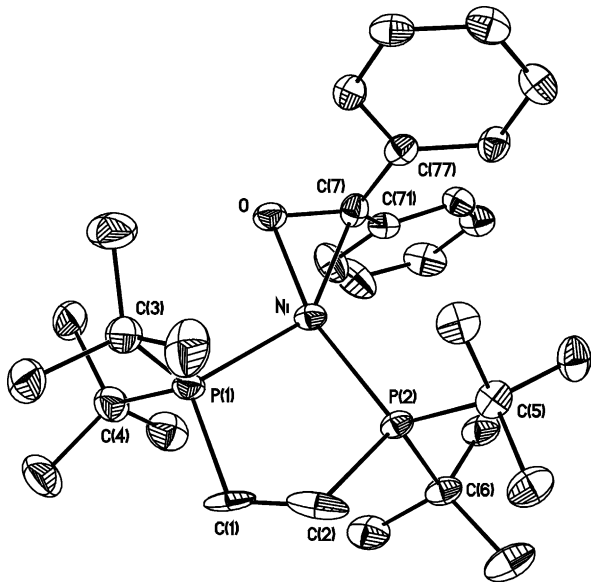

Fig. 7. A perspective view of **5** with thermal ellipsoids at the 35% probability level. Selected bond lengths (Å): Ni–O, 1.842(3); Ni–C(7), 1.997(5); O–C(7), 1.331(6); Ni–P(1), 2.199(2); Ni–P(2), 2.170(2). Selected angles (°): O–Ni–C(7), 40.31(17); P(1)–Ni–P(2), 92.46(6); C(7)–Ni–P(2), 123.37(14); O–Ni–P(1), 103.86(11).

were purchased from Acros or Fischer, stirred over sodium metal, and filtered through activated alumina. Azobenzene was recrystallized from Et_2O at −35 °C prior to usage. KC_8 and (dtbpe)$NiCl_2$ were prepared according to the literature [17,1r]. Phenylacetylene was distilled under vacuum and filtered through alumina prior to usage. LiC≡CPh was prepared by deprotonation of HC≡CPh with *n*-BuLi in hexanes at −35 °C. All other chemicals were used as received. IR data (Fluorolube S-20 or Nujol mulls, CaF_2 or KBr plates) were measured with a Nicolet 670-FT-IR instrument. Elemental analysis was performed by Desert Analytics (Tucson, AZ). ^1H, ^{13}C, and ^{31}P NMR spectra were recorded on Bruker 500 and 400 MHz NMR spectrometers. ^1H and ^{13}C NMR data are reported with reference to solvent resonances (residual C_6D_5H in C_6D_6, 7.16 and 128.0 ppm; residual $CHDCl_2$ in CD_2Cl_2, 5.32 and 53.8 ppm). ^{31}P NMR spectra were reported with respect to external 85% H_3PO_4 (0 ppm). Solution magnetic susceptibilities were determined by the method of Evans [18,19]. Room temperature (r.t.) X-band EPR spectra were recorded on a Bruker EMX spectrometer.

SQUID measurements were performed on a Quantum Designs SQUID magnetometer running MPMSR2 software (Magnetic Property Measurement System Revision 2). Data were recorded at 5000 G. Samples were suspended in the magnetometer in plastic straws sealed under nitrogen with Lilly No. 4 gel caps. Loaded samples were centered within the magnetometer using the DC centering scan at 35 K and 5000 G. Data were acquired at 10–20 (one data point per 2 K) and 20–255

K (one data point per 5 K) for sample **1**. Data were collected at 60–300 K for [**1**][PF_6] (one data point per 5 K).

The molar magnetic susceptibility (χ_M) was calculated by converting the calculated magnetic susceptibility (χ) obtained from the magnetometer to a molar susceptibility (using the multiplication factor {(molecular weight)/[(sample weight)*(Field Strength)]}). The magnetic susceptibility was adjusted for diamagnetic contributions using the constitutive corrections of Pascal's constants and a fixed temperature independent paramagnetism (TIP) crudely set to 1×10^{-4} cm^3 mol^{-1}. Curie–Weiss behavior was verified for [**1**][PF_6] by a plot of χ_m^{-1} versus T. Data were analyzed using the following relationships for [**1**][PF_6]: $\chi_m = \chi M/mG$; $\mu_{eff} = (7.997\chi_m T)^{1/2}$. These additional equations were used in calculating the antiferromagnetism of **1**: $|J|/kT_{max} = 1.599$; $\chi = 2Ng^2B^2/(kT[3+e^{(-J/kT)}])$.

3.2. Synthetic protocols

3.2.1. Synthesis of [(dtbpe)NiCl]$_2$ (**1**)

The following procedure is a slight modification and complement to the protocol from our original communication [1n]. (dtbpe)$NiCl_2$ (2.50 g, 5.58 mmol) was dissolved in 100 ml of THF and the dark-red solution was cooled to −35 °C. To the Ni precursor solution was added dropwise a suspension of KC_8 (840 mg, 6.22 mmol) in 20 ml of cold THF, causing immediate darkening of the solution and formation of graphite. After stirring for 1.5 h the solution was filtered and the filtrate dried under reduced pressure. The red–orange residue was extracted with approximately 160 ml of $C_6H_5CH_3$, filtered, and the solids washed with an additional 40 ml of $C_6H_5CH_3$. The filtrate was concentrated to approximately 25 ml and the solution cooled and stored at −35 °C for 1 day to afford large red blocks of pure **1** (1.32 g, 1.62 mmol, 59%) in one crop. The filtrate can be dried under vacuum and washed with 10 ml of cold petroleum ether/Et_2O (3:1) to afford an additional 316 mg of crude product (total yield, 73%). ^{1}H NMR (22 °C, 400 MHz, C_6D_6): δ 10.05 (br, $\Delta\nu_{1/2}$ = 600 Hz, C(CH_3)$_3$, 36 H), −7.90 (br, $\Delta\nu_{1/2}$ = 216 Hz, CH_2CH_2, 4 H) ppm. IR (Fluorolube mull, CaF_2): 2776(w), 2712(w), 1410(m), 1389(s), 1362(s) cm^{-1}. SQUID: $10 < T < 255$ K; $T_{max} = 32$ K; $J = -35$ cm^{-1}; modeled with $g = 2.05$. Solution $\mu_{eff} = 2.29\mu_B$ (per Ni center, C_6D_6, 22 °C, Evans's method). Solution molecular weight measurement by the Signer method (THF): average MW = 530 g mol^{-1}. EPR ($C_6H_5CH_3$, 25 °C): $g_{iso} = 2.141$, $A_{iso} = 73$ G (^{31}P, $n = 2$, 100%), linewidth: 37 G, $\nu = 9.766$ GHz, $p = 50.4$ mW, MA = 1 G, MF = 100 kHz. M.p. (dec.) 230–233 °C. *Anal*. Calc. for $C_{36}H_{80}Cl_2Ni_2P_4$: C, 52.4; H, 9.77. Found: C, 52.4; H, 9.95%.

3.2.2. Synthesis of [(dtbpe)NiCl]$_2$[PF_6] ([**1**][PF_6])

To a −35 °C slurry of **1** (74 mg, 0.0897 mmol) in 6 ml of THF was added dropwise a cooled 4 ml THF suspension of [$FeCp_2$][PF_6] (30 mg, 0.0897 mmol). The stirred solution slowly turned purple in color. After 1.5 h of stirring, the solution was filtered and pure crystals of [**1**][PF_6] were obtained by slow crystallization from a THF/Et_2O solution at −35 °C (82 mg, 0.0845 mmol, 94% yield). ^{1}H NMR (22 °C, 500.1 MHz, CD_2Cl_2): δ 5.60 (br, $\Delta\nu_{1/2}$ = 260 Hz, C(CH_3)$_3$, 36 H), −6.00 (br, $\Delta\nu_{1/2}$ = 280 Hz, CH_2CH_2, 4 H). IR (Nujol mull, KBr): 1178 (s), 1019 (m), 937 (s) 840 (s), 722 (w), 695 (w) 667 (w), 558 (m) 500 (m) cm^{-1}. $\mu_{eff} = 2.25\mu_B$ (CD_2Cl_2, 298 K, Evans' method). SQUID: $60 < T < 300$ K; $\mu_{eff\ (avg)} = 1.96\mu_B$ (dimer). EPR (THF, 25 °C): $g_{iso} = 2.158$, $A_{iso} = 61$ G (^{31}P, $n = 2$, 100%), linewidth: 52 G, ν = 9.751 GHz, $p = 50.3$ mW, MA = 1 G, MF = 100 kHz. *Anal*. Calc. for $C_{36}H_{80}F_6Ni_2P_5$: C, 44.6; H, 8.31. Found: C, 44.0; H, 8.01%.

3.2.3. Synthesis of (dtbpe)Ni(NO)Cl (**2**)

In a 100 ml Schlenk flask a solution of 1 (315 mg, 0.382 mmol) in 30 ml of $C_6H_5CH_3$ was degassed and cooled to −78 °C. Nitric oxide (19.62 ml, 1 atm, 2.10 equivalent) was added via syringe causing a rapid color change to blue with precipitation of a blue solid. After 1.5 h the suspension was concentrated to half its original volume and taken into the glovebox. The solution was then cooled to −35 °C for 2 h, filtered, and the blue solid washed with Et_2O, and dried under vacuum to afford crude **2** (289 mg, 0.653 mmol, 86% yield). Large blue blocks of **2** were grown from a CH_2Cl_2 solution layered with excess Et_2O, and cooled to −35 °C for 2 days (270 mg, 0.611 mmol, 80% yield). ^{1}H NMR (22 °C, 500.1 MHz, CD_2Cl_2): δ 2.15 (m, CH_2CH_2, 2 H), 1.86 (m, CH_2CH_2, 2 H), 1.35 (d, C(CH_3)$_3$, J_{HP} = 12 Hz, 18 H), 1.26 (d, C(CH_3)$_3$, J_{HP} = 12 Hz, 18 H). ^{13}C{^{1}H} NMR (22 °C, 125.8 MHz, CD_2Cl_2): δ 36.53 (bs, $C(CH_3)_3$), 36.05 (bs, $C(CH_3)_3$), 30.58 (s, C(CH_3)$_3$), 30.11 (s, C(CH_3)$_3$), 21.84 (t, CH_2CH_2, J_{CP} = 14 Hz). ^{31}P{^{1}H} NMR (22 °C, 202.4 MHz, CD_2Cl_2): δ 92.66 (s, $P((C(CH_3)_3)_2)$. IR (Fluorolube, CaF_2): 2993(m), 2948(m), 2865(s), 1734(s, ν_{NO}), 1393(w), 1372(w), 1364(w) cm^{-1}. *Anal*. Calc. for $C_{18}H_{40}ClNNiOP_2$: C, 48.8; H, 9.11; N, 3.16. Found: C, 48.8; H, 9.32; N, 3.09%.

3.2.4. Synthesis of (dtbpe)Ni(Cl)(O,N:η^2-TEMPO) (**3**)

To a −35 °C 5 ml $C_6H_5CH_3$ solution of **1** (68 mg, 0.082 mmol) was added dropwise a cold $C_6H_5CH_3$ solution of TEMPO (26 mg, 0.165 mmol) causing a rapid color change from pale orange to purple. The solution was stirred for 1 h, filtered, and dried under vacuum. The solid was extracted with Et_2O, filtered, concentrated, and cooled to −35 °C for 1 day. Large

purple blocks formed, which were filtered, washed with cold petroleum ether, and dried under vacuum to afford pure **3** (85 mg, 0.149 mmol, 90% yield). ^{1}H NMR (22 °C, 500.1 MHz, C_6D_6): δ 3.07 (s, ON–2,2,6,6-(CH_3)$_4$C$_4$H$_6$, 6H), 2.24 (m, CH_2CH_2, 2H), 2.13 (m, ON–2,2,6,6-(CH$_3$)$_4$C$_5$$H_6$, 2H), 1.77 (m, C$H_2CH_2$, 2H), 1.38 (d, C(C$H_3$)$_3$, J_{HP} = 13 Hz, 18H), 1.27 (m, ON–2,2,6,6-(CH$_3$)$_4$C$_5$$H_6$, 2H), 1.26 (d, C(C$H_3$)$_3$, J_{HP} = 10 Hz, 18 H), 1.10 (m, ON–2,2,6,6-(CH$_3$)$_4$C$_5$$H_6$, 2H), 1.05 (s, ON–2,2,6,6-(CH_3)$_4$C$_4$H$_6$, 6H). ^{13}C{^{1}H} NMR (22 °C, 125.8 MHz, C_6D_6): δ 37.48 (s, C(CH$_3$)$_2$), 34.07 (d, C(CH$_3$)$_2$, J_{CP} = 14 Hz), 32.88 (s, C(CH$_3$)$_2$), 31.79 (d, C(CH$_3$)$_2$, J_{CP} = 23 Hz), 30.03 (s, CH$_2$), 29.92 (s, C(CH$_3$)$_3$), 23.71 (s, CH$_2$), 22.39 (m, CH$_2C$H$_2$, J_{CP} = 13 Hz), 22.10 (d, CH$_2C$H$_2$, J_{CP} = 13 Hz), 19.28 (d, C(CH$_3$)$_2$, J_{CP} = 23 Hz). ^{31}P{^{1}H} NMR (22 °C, 202.4 MHz, C_6D_6): δ 52.27 (d, P(C(CH$_3$)$_3$)$_2$, J_{PP} = 33 Hz), 37.65 (d, P(C(CH$_3$)$_3$)$_2$, J_{PP} = 31 Hz). *Anal*. Calc. for $C_{27}H_{58}ClNNiOP_2$: C, 56.3; H, 10.2; N, 2.52. Found: C, 56.7; H, 10.3; N, 2.22%.

3.2.5. Synthesis of (dtbpe)Ni(SPh)Cl (4)

In a vial was dissolved 1 (104 mg, 0.126 mmol) in 7 ml of $C_6H_5CH_3$ and the solution cooled to −35 °C. To the cold solution was added dropwise a cold $C_6H_5CH_3$ (5 ml) solution containing diphenyldisulfide (28 mg, 0.126 mmol) causing a slow color change from pale orange to brown. The solution was stirred for 24 h, filtered, and dried under vacuum. The solids were extracted with a minimum of CH_2Cl_2, filtered, layered with excess Et_2O, and cooled to −35 °C overnight. Large brown blocks form, which were filtered, washed with Et_2O, and dried under vacuum to afford 4 (78 mg, 0.150 mmol, 60% yield). ^{1}H NMR (22 °C, 500.1 MHz, CD_2Cl_2): δ 7.48 (d, o-C$_6$H$_5$, 2H), 7.00 (t, m-C$_6$H$_5$, 2H), 6.93 (t, p-C$_6$H$_5$, 1H), 1.74 (m, CH_2CH_2, 4H), 1.56 (s, C(CH_3)$_3$, 18H), 1.55 (s, C(CH_3)$_3$, 18H). ^{13}C{^{1}H} NMR (22 °C, 125.8 MHz, CD_2Cl_2): δ 144.2 (s, aryl), 135.2 (s, aryl), 127.1 (s, aryl), 122.7 (s, aryl), 38.03 (bs, C(CH$_3$)$_3$), 31.04 (s, C(CH$_3$)$_3$), 30.91 (s, C(CH$_3$)$_3$), 21.84 (bs, CH$_2C$H$_2$). ^{31}P{^{1}H} NMR (22 °C, 202.4 MHz, CD_2Cl_2): δ 90.05 (bs, P(C(CH$_3$)$_3$)$_2$, $\Delta\nu_{1/2}$ = 270 Hz), 81.84 (bs, P(C(CH$_3$)$_3$)$_2$, $\Delta\nu_{1/2}$ = 30 Hz).

3.2.6. Synthesis of (dtbpe)Ni(η^2-OCPh$_2$) (5)

In a vial containing benzophenone (49 mg, 0.269 mmol) dissolved in 10 ml of THF was added small strips of sodium metal (20 mg, 0.870 mmol) causing a slow color change to purple. The solution was vigorously stirred for 4 h, filtered, cooled to −35 °C, and added dropwise to a cold THF (10 ml) solution containing **1** (110 mg, 0.134 mmol) causing a rapid color change to brown–green. The reaction mixture was allowed to stir for 2 h, filtered and dried under reduced pressure. The solids were extracted with $C_6H_5CH_3$, filtered to remove a brown tar, and dried to give an orange powder of crude **5** [151 mg, 0.254 mmol, 96% yield]. Large orange blocks of pure **5** are obtained by dissolving the orange powder in a minimum of CH_2Cl_2, filtering the solution, layering carefully with excess Et_2O, and cooling the layered solution to −35 °C for 2 days. The crystals and solids were filtered, washed with Et_2O, and dried under vacuum to afford pure product (141 mg, 0.237 mmol, 88% yield). ^{1}H NMR (22 °C, 500.1 MHz, CD_2Cl_2): δ 7.93 (d, o-C$_6$H$_5$, 4 H), 7.15 (t, m-C$_6$H$_5$, 4 H), 7.06 (t, p-C$_6$H$_5$, 2 H), 1.59 (m, CH_2CH_2, 4 H), 1.41 (d, C(CH_3)$_3$, J_{HP} = 8 Hz, 18 H), 0.91 (d, C(CH_3)$_3$, J_{HP} = 13 Hz, 18 H). ^{13}C{^{1}H} NMR (22 °C, 125.8 MHz, CD_2Cl_2): δ 148.7 (s, aryl), 127.7 (s, aryl), 127.1 (s, aryl), 123.5 (s, aryl), 34.80 (d, C(CH$_3$)$_3$, J_{CP} = 12 Hz), 34.48 (bs, C(CH$_3$)$_3$), 30.71 (d, C(CH$_3$)$_3$, J_{PC} = 4 Hz), 30.49 (d, C(CH$_3$)$_3$, J_{CP} = 4 Hz), 24.92 (t, CH$_2C$H$_2$, J_{CP} = 20 Hz), 20.04 (t, CH$_2C$H$_2$, J_{CP} = 13 Hz) (Note: The ketone carbon resonance OCPh$_2$ could not be located in the ^{13}C NMR spectrum.). ^{31}P{^{1}H} NMR (22 °C, 202.4 MHz, CD_2Cl_2): δ 88.99 (d, P(C(CH$_3$)$_3$)$_2$, J_{PP} = 66 Hz), 82.65 (d, P(C(CH$_3$)$_3$)$_2$, J_{PP} = 66 Hz). *Anal*. Calc. for $C_{31}H_{50}NiOP_2$: C, 66.6; H, 9.01. Found: C, 66.4; H, 9.23%.

3.2.7. Synthesis of (dtbpe)Ni(η^2-N$_2$Ph$_2$) (6)

KC_8 (54 mg, 0.399 mmol) and PhN=NPh (69 mg, 0.379 mmol) were mixed as solids in a 100 ml Schlenk flask, and onto the solids was vacuum transferred approximately 20 ml of dry THF at −78 °C. The mixture was stirred for 2 h at −78 °C under N_2 to generate in situ the azobenzene radical anion (green–brown solution with a black graphite precipitate). In a separate 100 ml Schlenk flask equipped with a stir bar was dissolved **1** (156 mg, 0.189 mmol) in 15 ml of THF. The pale orange solution was cooled to −78 °C and transferred via cannula (added slowly and dropwise) to the radical anion mixture at −78 °C. After 1 h the suspension was allowed to warm to r.t., stirred for an additional 2 h, and taken into the glovebox. The solution was filtered, extracted with $C_6H_5CH_3$, and dried under vacuum to afford crude **6** (206 mg, 0.368 mmol, 97% yield) as a dark red powder. Large red blocks of **6** were obtained by extracting the solids with $C_6H_5CH_3$, filtrating the red solution, concentrating the solution, adding 5 ml of Et_2O, and cooling the solution overnight. The crystals and solids were collected in three crops, washed with cold Et_2O, and dried under reduced pressure (178 mg, 0.318 mmol, 84% yield). ^{1}H NMR (22 °C, 500.1 MHz, CD_2Cl_2): δ 7.63 (d, o-C$_6$H$_5$, 4 H), 7.09 (t, m-C$_6$H$_5$, 4H), 6.82 (t, p-C$_6$H$_5$, 2H), 1.53 (bs), 0.85 (bs). ^{13}C{^{1}H} NMR (22 °C, 125.8 MHz, CD_2Cl_2): δ 159.1 (s, aryl), 128.7 (s, aryl), 122.5 (s, aryl), 120.2 (s, aryl), 34.64 (bs, C(CH$_3$)$_3$), 30.86 (s, C(CH$_3$)$_3$), 22.20 (t, CH$_2$CH$_2$, J_{CP} = 16 Hz). ^{31}P{^{1}H} NMR (22 °C, 202.4 MHz, CD_2Cl_2): δ 81.0 (s, P(C(CH$_3$)$_3$)$_2$). *Anal*. Calc. for

$C_{30}H_{50}N_2NiP_2$: C, 64.4; H, 9.01; N, 5.01. Found: C, 64.7; H, 9.26; N, 4.73%.

3.2.8. Synthesis of [(dtbpe)Ni(C,C′:η^2-CCPh)]$_2$ (7)

To a cold (−35 °C) 8 ml Et_2O suspension of **1** (148 mg, 0.179 mmol) was added a 3 ml ether solution containing LiC≡CPh (39 mg, 0.358 mmol). The solution gradually turned yellow–orange and became homogeneous. After 24 h of stirring at r.t., the solution was filtered, concentrated to 4 ml and cooled to give crystals of **7** (160 mg, 0.169 mmol, 94%). ^{1}H NMR (22 °C, 400 MHz, C_6D_6): δ 7.64 (d, aryl, 2H), 7.27 (d, aryl, 2H), 6.96 (d, aryl, 1H), 1.59 (m, CH_2CH_2, 4H), 1.39 (d, C(CH_3), 9H), 1.29 (d, C(CH_3), 9H), 1.04 (t, C(CH3), 18H). ^{13}C{^{1}H} NMR (22 °C, 125.8 MHz, C_6D_6): δ 145.2 (s, aryl), 132.6 (bs, *C*=*C*), 132.2 (bs, *C*=*C*), 127.5 (s, aryl), 127.2 (s, aryl), 122.9 (s, aryl), 35.3 (s, *C*(CH$_3$)$_3$, J_{CP} = 10 Hz), 34.3 (s, *C*(CH$_3$)$_3$, J_{CP} = 10 Hz), 33.8 (s, C(*C*H$_3$)$_3$, 31.3 (s, C(*C*H$_3$)$_3$, 31.0 (s, C(*C*H$_3$)$_3$, 30.2 (s, C(*C*H$_3$)$_3$, 23.9 (m, *C*H$_2$*C*H$_2$), 22.6 (m, *C*H$_2$*C*H$_2$). ^{31}P{^{1}H} NMR (22 °C, 202.4 MHz, C_6D_6): δ 96.6 (m, P(C(CH$_3$)$_3$)$_2$, J_{PP} = 46, 21 Hz). IR (Nujol mull, KBr): 1589 (s), 1304 (w), 1178 (s), 1019 (m), 952 (w), 847 (s), 813 (w), 753 (m), 722 (m), 696 (w), 673 (w), 663 (w), 601 (w), 565 (w), 546 (w) cm^{-1}. *Anal*. Calc. for $C_{52}H_{90}Ni_2P_4$: C, 65.3; H, 9.48. Found: C, 64.6; H, 9.64%.

3.3. Crystallographic structural determinations

In a typical procedure a single crystal of **1**, [**1**][PF_6], **3**, or **5** was selected under a stereo-microscope while immersed in Paratone oil to minimize possible reaction with air. The crystal was removed from the oil using a tapered fiber that also served to hold the crystal for data collection. The crystal was mounted and centered on a Bruker SMART APEX system. Rotation and still images showed diffractions to be sharp. Frames separated in reciprocal space were obtained and provided an orientation matrix and initial cell parameters. Final cell parameters were obtained from the full data set. A hemisphere data set was obtained which samples approximately 1.2 hemispheres of reciprocal space to a resolution of 0.84 Å using 0.3° steps in ω. Data collection was made at 100 K. Integration of intensities and refinement of cell parameters were done using SAINT. Absorption corrections were applied using psi-scans. Observation after 5.5 h of data collection suggested no decomposition of the crystal. Structures were solved by direct methods using the SHELXTL (version 5.1) program library [20]. Space groups were based on systematic absences and intensity statistics and hydrogen atoms were treated as idealized contributions.

3.4. EPR measurements

In a typical experiment a $C_6H_5CH_3$ or THF solution containing **1** or [**1**][PF_6] (concentration ranging from 0.1 to 30 mM) were collected at 278 K. The magnitude of the P ($n = 2$) coupling in **1** was found by simulation to be 73 G and for [**1**][PF_6] was 61 G, a value typical for Ni(I) complexes bearing two phosphorus nuclei [1l,1n]. g_{iso} values of 2.14 and 2.16 for **1** and [**1**][PF_6], respectively, also fall within reported results [21].

4. Conclusions

The dimeric nickel(I) complex **1** has been prepared and characterized. Chemistry associated with complex **1** include its one electron oxidation to prepare the dimeric cationic complex [**1**][PF_6], radical coupling with NO and TEMPO to afford the diamagnetic adducts **2** and **3**, reduction of the S–S bond of diphenyldisulfide to give the Ni(II) thiolato complex **4**, and ligand metathesis along with radical coupling to afford products **5**, **6**, and **7**. The chemistry reported in this paper provides classic examples of the rich redox chemistry offered by Ni(I).

5. Supplementary material

Crystallographic data for the structural analysis have been deposited with the Cambridge Crystallographic Data Centre, CCDC Nos. 187549–187551, and 187553 for compounds **1**, [**1**][PF_6], **3**, and **5**, respectively. Copies of this information may be obtained free of charge from The Director, CCDC, 12 Union Road, Cambridge, CB2 1EZ, UK (fax: +44-1223-336-033; e-mail: deposit@ccdc.cam.ac.uk or www: http://www.ccdc.cam.ac.uk). The deposited information contains atomic coordinates, anisotropic displacement parameters, tables of bond distances and angles, hydrogen coordinates, and torsion angles. Structure factor tables may be obtained from the authors.

Acknowledgements

We are grateful to the National Science Foundation for financial support of this research through a grant to G.L.H. D.J.M. acknowledges postdoctoral fellowship support from the Ford Foundation and the National Institutes of Health. R.W. thanks the Department of Education for a GAANN Fellowship, and D.M.J. acknowledges the N.S.F. for a predoctoral fellowship. Joshua Figueroa and Professor Karsten Meyer are thanked for assistance in recording and simulating EPR spectra, respectively.

References

[1] For literature pertinent to Ni(I) complexes see: (a) D.C. Bradley, M.B. Hursthouse, R.J. Smallwood, A.J. Welch, J. Chem. Soc., Chem. Commun. (1972) 872;
(b) A. Bencini, C. Benelli, D. Gatteschi, L. Sacconi, Inorg. Chim. Acta 37 (1979) 195;
(c) A. Bencini, C. Benelli, D. Gatteschi, L. Sacconi, Inorg. Chim. Acta 29 (1978) L243;
(d) P. Dapporto, L. Sacconi, Inorg. Chim. Acta 39 (1980) 61;
(e) F. Cecconi, S. Midollini, A. Orlandini, J. Chem. Soc., Dalton Trans. (1983) 2263;
(f) H. Schafer, D. Binder, B. Deppisch, G. Mattern, Z. Anorg. Allg. Chem. 79 (1987) 79;
(g) P. Stavropoulos, M.C. Muetterties, M. Carrié, R.H. Holm, J. Am. Chem. Soc. 113 (1991) 8485;
(h) P. Ge, C.G. Riordan, G.P.A. Yap, A.L. Rheingold, Inorg. Chem. 35 (1996) 5408;
(i) T.L. James, L.S. Cai, M.C. Muetterties, R.H. Holm, Inorg. Chem. 35 (1996) 4148;
(j) D.A. Vicic, W.D. Jones, J. Am. Chem. Soc. 121 (1999) 4070;
(k) D.A. Vicic, W.D. Jones, J. Am. Chem. Soc. 121 (1999) 7606;
(l) F. Scott, C. Krüger, P. Betz, J. Organomet. Chem. 387 (1990) 113;
(m) L. Gomez, E. Pereira, B. de Castro, J. Chem. Soc., Dalton Trans. (2000) 1373;
(n) D.J. Mindiola, G.L. Hillhouse, J. Am. Chem. Soc. 123 (2001) 4623;
(o) P.J. Schebler, B.S. Mandimutsira, C.G. Riordan, L. M, Liable-Sands, C.D. Incarvito, A.L. Rheingold, J. Am. Chem. Soc. 123 (2001) 331;
(p) B.S. Mandimutsira, J.L. Yamarik, T.C. Brunold, W. Gu, S.P. Cramer, C.G. Riordan, J. Am. Chem. Soc. 123 (2001) 9194;
(q) R. Melenkivitz, D.J. Mindiola, G.L. Hillhouse, J. Am. Chem. Soc. 124 (2002) 3846;
(r) I. Bach, R. Goddard, C. Kopiske, K. Seevogel, K.-R. Pörschke, Organometallics 18 (1999) 10;
(s) A. Bakac, J.H. Espenson, J. Am. Chem. Soc. 108 (1986) 713;
(t) N. Sadler N, S.L. Scott, A. Bakac, J.H. Espenson, M.S. Ram, Inorg. Chem. 28 (1989) 3951;
(u) M.S. Ram, A. Bakac, J.H. Espenson, Inorg. Chem. 25 (1986) 3267;
(v) E.K. Barefield, D.A. Krost, D.S. Edwards, D.G. Van Derveer, R.L. Trytko, S.P. O'Rear, J. Am. Chem. Soc. 103 (1981) 6219;
(w) M.J. D'Aniello, Jr., E.K. Barefield, J. Am. Chem. Soc. 100 (1978) 1474;
(x) D.L. DeLaet, D.R. Powell, C.P. Kubiak, Organometallics 4 (1985) 954.

[2] (a) R.P. Hausinger, Biochemistry of Nickel, Plenum, New York, 1993;
(b) R.P. Hausinger, JBIC 2 (1997) 279;
(c) V.J. DeRose, J. Telser, M.E. Anderson, P.A. Lindahl, B.M. Hoffman, J. Am. Chem. Soc. 120 (1998) 8767;
(d) R.K. Thauer, Science 293 (1990) 1264.

[3] S. Fox, R.T. Stibrany, J.A. Potenza, H.J. Schugar, Inorg. Chim. Acta 316 (2001) 122.

[4] (a) D. Berglund, D.W. Meek, Inorg. Chem. 11 (1972) 1493;
(b) J.H. Meihners, C.J. Rix, J.C. Clardy, J.G. Verkade, Inorg. Chem. 14 (1975) 705;
(c) G. Elbaze, F. Dahan, M. Dartiguenave, Y. Dartiguenave, Inorg. Chim. Acta 87 (1984) 91;
(d) A. Del Zotto, A. Mezzetti, V. Novelli, P. Rigo, M. Lanfranchi, A. Tiripicchio, J. Chem. Soc., Dalton Trans. (1990) 1035;
(e) A.F.M.M. Rahman, G. Salem, F.S. Stephens, S.B. Wild, Inorg. Chem. 29 (1990) 5225.

[5] M.K. Mahanthappa, K.W. Huang, A.P. Cole, R.M. Waymouth, Chem. Commun. (2002) 502.

[6] For a recent article on η^2-binding of TEMPO in metal complexes, see: W.J. Evans, J.M. Perotti, R.J. Doedens, J.W. Ziller, Chem. Commun. (2001) 2326.

[7] M. Wedler, M. Noltemeyer, U. Pieper, H.-G. Schmidt, D. Stalke, F.T. Edelmann, Angew. Chem., Int. Ed. Engl. 29 (1990) 894.

[8] F.A. Neugebauer, H. Weger, Chem. Ber. 108 (1975) 2703.

[9] (a) R. Countryman, B.R. Penfold, J. Cryst. Mol. Struct. 2 (1972) 281;
(b) T.T. Tsou, J.C. Huffman, J.K. Kochi, Inorg. Chem. 18 (1979) 2311;
(c) R.S. Dickson, J.A. Ibers, J. Am. Chem. Soc. 94 (1972) 2988;
(d) S.D. Ittel, J.A. Ibers, J. Organomet. Chem. 57 (1973) 389.

[10] D.J. Mindiola, K. Kitiachvili, R. Waterman, G.L. Hillhouse, manuscript in preparation.

[11] R. Waterman, G.L. Hillhouse, unpublished results.

[12] U. Rosenthal, H. Gorls, J. Organomet. Chem. 348 (1988) 135.

[13] A preliminary X-ray structural analysis confirms this connectivity.

[14] A search in the Cambridge Structural Database shows crystallized benzophenone to have a C=O bond length between 1.224 and 1.238 Å.

[15] For a general description of the equipment and techniques, see: B.J. Burger, J.E. Bercaw, in: A.L. Wayda, M.Y. Darensbourg (Eds.), Experimental Organometallic Chemistry, ACS Symposium Series 357, American Chemical Society, Washington, DC, 1987, pp. 79–98.

[16] A.B. Pangborn, M.A. Giardello, R.H. Grubbs, R.K. Rosen, F.J. Trimmers, Organometallics 15 (1996) 1518.

[17] M. Schwindt, T. Lejon, L. Hegedus, Organometallics 9 (1990) 2814.

[18] S.K. Sur, J. Magn. Reson. 82 (1989) 169.

[19] D.F. Evans, J. Chem. Soc. (1959) 2003.

[20] G. Sheldrick, SHELXTL, Version 5.1, Bruker-Siemens Analytical X-ray Systems, Madison, WI, 1997.

[21] (a) V.V. Saraev, P.B. Kraikivskii, P.G. Lazarev, G. Myagmarsuren, V.S. Tkach, F.K. Shmidt, Russ. J. Coord. Chem. 22 (1996) 655;
(b) V.V. Saraev, P.B. Kraikivskii, P.G. Lazarev, V.S. Tkach, F.K. Shmidt, Russ. J. Coord. Chem. 25 (1999) 220;
(c) V.V. Saraev, P.B. Kraikivskii, A.B. Zaitsev, V.S. Tkach, F.K. Shmidt, Russ. J. Coord. Chem. 26 (2000) 487.